Electronic Supplementary Material (ESI) for Physical Chemistry Chemical Physics.
This journal is © the Owner Societies 2024

Supplementary information

Exploration of 4-substituted thiophene-based azo dyes for Dye-sensitized solar cells and non-linear optical material: Synthesis and an in-silico approach

The theoretical background of DSSC

The power conversion efficiency (η_p) is well known to be one of the most parameters that characterize the performance of DSSC devices, and it is commonly determined through the open-circuit photovoltage (V_{OC}), short-circuit current density (J_{SC}), fill factor (FF), and incident solar power (P_{inc}), as shown below.[1–3]

$$\eta_p = \frac{J_{SC} V_{OC} FF}{P_{inc}} \quad (1)$$

The J_{SC} of DSSCs is influenced by both the dyes' absorption coefficient and how TiO_2 interacts with the sensitizers. The following equation can be used for calculating the J_{SC} [2,4]

$$J_{SC} = \int LHE\,(\lambda)\Phi_{inj}\eta_{coll}d\lambda \quad (2)$$

where **LHE** = light-harvesting efficiency at highest absorption maxima

Φ_{inj} = Electron injection efficiency

η_{coll} = Charge collection efficiency

when η_{coll} in a system is considered constant, the LHE (λ) is calculated as [2–5]

$$LHE = 1 - 10^{-f} \quad (3)$$

where **f** denotes the oscillator strength of dye at a particular wavelength. In contrast, Φ_{inj} is associated with the driving force ($\mathbf{G_{inject}}$) of electrons injected to the semiconductor from the dye's excited state, as discussed below [2–5]

$$\Phi_{inj} \propto (-\Delta G_{inject}) \quad (4)$$

where, $$\Delta G_{inject} = E_{ox}^{dye*} - E_{CB} \quad (5)$$

where E_{ox}^{dye*} is dyes' excited state oxidation potential and E_{CB} is the semiconductor (TiO_2) conduction band (E_{CB} (TiO_2) = - 4.0 eV). [2–5] E_{ox}^{dye*} of a dye can be calculated through the equation given below [2–5]

$$E_{ox}^{dye*} = E_{ox}^{dye} - E_{Vert} \quad (6)$$

where E_{ox}^{dye} is the dye's ground state oxidation potential energy and E_{Vert} is the vertical excitation energy associated with λ_{Vert}. E_{ox}^{dye} is defined as the negative of highest occupied molecular orbital energy ($\mathbf{E_{HOMO}}$).

Sensitizer's effectiveness in DSSC is impacted by the driving force of regeneration (ΔG_{reg}) energy since it directly affects the short circuit current (Jsc). The following equation can be used to determine ΔG_{reg} [5]

$$\Delta G_{reg} = E_{redox} - E_{ox}^{dye} \quad (7)$$

where E_{redox} is the electrolyte's redox potential i.e., I^-/I_3^- = -4.80 eV.

In DSSCs, Voc can be determined by the energy difference between dye's lowest unoccupied molecular orbital (LUMO) and E_{CB} as follows [2,3]

$$V_{OC} = E_{LUMO} - E_{CB} \quad (8)$$

here E_{LUMO} is the dyes LUMO energy.

SI Table 1 Computed bond lengths of SR1 to SR9 in gas phase optimized at B3LYP/6-111++G (d, p) level of theory

Dyes	N-C	C=C	C-C	C=C	C-N	N=N	N-C	C=C	C-C	C=C	C-C	C=O
	b_1 (Å)	b_2 (Å)	b_3 (Å)	b_4 (Å)	b_5 (Å)	b_6 (Å)	b_7 (Å)	b_8 (Å)	b_9 (Å)	b_{10} (Å)	b_{11} (Å)	b_{12} (Å)
SR1	1.348	1.403	1.416	1.373	1.353	1.267	1.409	1.382	1.382	1.405	1.506	1.205
SR2	1.348	1.401	1.425	1.382	1.349	1.270	1.407	1.406	1.382	1.406	1.505	1.206
SR3	1.349	1.401	1.430	1.390	1.347	1.271	1.406	1.406	1.382	1.406	1.505	1.206
SR4	1.348	1.401	1.432	1.394	1.343	1.274	1.406	1.409	1.379	1.409	1.475	1.221
SR5	1.349	1.400	1.434	1.398	1.339	1.276	1.404	1.410	1.378	1.409	1.473	1.221
SR6	1.349	1.400	1.433	1.394	1.343	1.274	1.404	1.407	1.381	1.406	1.504	1.206
SR7	1.349	1.400	1.433	1.394	1.343	1.274	1.405	1.407	1.382	1.406	1.504	1.206
SR8	1.348	1.400	1.432	1.394	1.344	1.273	1.405	1.407	1.381	1.406	1.504	1.206
SR9	1.350	1.400	1.429	1.386	1.349	1.270	1.407	1.406	1.382	1.406	1.505	1.206

SI Table 2 Computed bond lengths of SR1 to SR9 in DMF optimized at B3LYP/6-111++G (d, p) level of theory

Dyes	N-C	C=C	C-C	C=C	C-N	N=N	N-C	C=C	C-C	C=C	C-C	C=O
	b_1 (Å)	b_2 (Å)	b_3 (Å)	b_4 (Å)	b_5 (Å)	b_6 (Å)	b_7 (Å)	b_8 (Å)	b_9 (Å)	b_{10} (Å)	b_{11} (Å)	b_{12} (Å)
SR1	1.335	1.413	1.411	1.377	1.348	1.273	1.407	1.408	1.380	1.407	1.493	1.215
SR2	1.336	1.410	1.421	1.386	1.344	1.274	1.407	1.403	1.385	1.403	1.489	1.209
SR3	1.335	1.411	1.425	1.392	1.343	1.276	1.405	1.409	1.380	1.407	1.492	1.215
SR4	1.335	1.410	1.427	1.395	1.340	1.278	1.404	1.410	1.380	1.408	1.491	1.216
SR5	1.336	1.409	1.431	1.403	1.334	1.283	1.400	1.411	1.380	1.408	1.489	1.216
SR6	1.336	1.410	1.428	1.398	1.339	1.279	1.403	1.410	1.380	1.408	1.491	1.216
SR7	1.336	1.410	1.428	1.397	1.339	1.279	1.403	1.408	1.380	1.408	1.491	1.216
SR8	1.335	1.410	1.427	1.395	1.341	1.278	1.403	1.410	1.380	1.408	1.491	1.215
SR9	1.335	1.411	1.423	1.388	1.345	1.274	1.406	1.409	1.380	1.407	1.492	1.215

SI Table 3 Computed HOMO, LUMO, gap, dipole moment, μ, η, ω, and Γ of SR1 to SR9 optimized at B3LYP/6-311++G (d, p) level of theory

Dyes	**Phase**	**HOMO-1**	**HOMO**	**LUMO**	**GAP***	**μ**	**η**	**ω**	**Γ**	**Dipole Moment**
		eV	eV	eV	eV	eV	eV	eV	eV	Debye
SR1	Vacuum	-7.247	-6.375	-3.284	3.091	4.830	1.546	7.546	2.220	9.387
	DMF	-7.075	-6.108	-3.118	2.990	4.613	1.495	7.117	2.023	13.675
SR2	Vacuum	-7.141	-6.267	-3.164	3.103	4.715	1.551	7.167	2.228	9.000
	DMF	-6.955	-6.003	-2.992	3.011	4.497	1.505	6.718	2.059	10.889
SR3	Vacuum	-7.023	-6.211	-3.232	2.979	4.721	1.489	7.483	2.167	8.253
	DMF	-6.933	-6.041	-3.138	2.903	4.590	1.452	7.255	2.012	12.442
SR4	Vacuum	-6.574	-6.023	-3.165	2.858	4.594	1.429	7.383	2.307	5.108
	DMF	-6.534	-5.954	-3.098	2.856	4.526	1.428	7.172	2.275	10.959
SR5	Vacuum	-6.137	-5.567	-3.001	2.566	4.284	1.283	7.153	1.997	4.242
	DMF	-6.077	-5.510	-3.027	2.483	4.268	1.242	7.337	1.915	9.795
SR6	Vacuum	-6.151	-5.533	-3.108	2.425	4.320	1.212	7.697	1.807	7.089
	DMF	-6.058	-5.515	-3.097	2.418	4.306	1.209	7.670	1.876	11.051
SR7	Vacuum	-6.165	-5.799	-3.054	2.745	4.427	1.373	7.139	2.379	7.282
	DMF	-6.104	-5.779	-3.071	2.708	4.425	1.354	7.231	2.382	11.275
SR8	Vacuum	-6.157	-5.554	-3.149	2.404	4.352	1.202	7.876	1.801	6.105
	DMF	-6.064	-5.580	-3.120	2.460	4.350	1.230	7.691	1.976	9.562
SR9	Vacuum	-6.264	-5.834	-3.189	2.645	4.512	1.323	7.694	2.216	8.021
	DMF	-6.119	-5.858	-3.139	2.719	4.498	1.359	7.443	2.457	12.392

*GAP = LUMO-HOMO

SI Table 4 Simulated λ_{vert}, E_{vert}, f, LHE, τ_0 and % OC of SR1 to SR9 at TD-DFT/CAM-B3LYP/6-311++G (d, p) level of theory

Dyes	λ_{vert} (nm)		E_{Vert} (eV)		*f*		LHE		τ_0 (sec)		% OC*	
	Vacuum	DMF	Vacuum	DMF	Vacuum	DMF	Vacuum	DMF	Vacuum	DMF	Vacuum	DMF

SR1	371.55	423.99	3.337	2.924	0.939	1.223	0.885	0.940	0.143	0.143	95.22	89.69
SR2	372.85	426.04	3.325	2.910	0.943	1.270	0.886	0.946	0.144	0.139	95.40	92.11
SR3	387.89	438.80	3.196	2.826	0.827	1.169	0.851	0.932	0.177	0.161	95.78	92.36
SR4	397.13	445.48	3.122	2.783	0.767	1.161	0.829	0.931	0.200	0.167	95.59	95.55
SR5	428.74	476.28	2.892	2.603	0.333	0.943	0.536	0.886	0.538	0.235	59.69	81.20
SR6	429.22	461.57	2.889	2.686	0.342	0.958	0.545	0.890	0.526	0.217	54.82	56.90
SR7	426.51	452.58	2.907	2.740	0.068	0.981	0.144	0.896	2.624	0.204	18.62	74.21
SR8	425.75	451.11	2.912	2.748	0.082	1.070	0.172	0.915	2.153	0.186	20.37	50.17
SR9	426.42	436.85	2.908	2.838	0.031	1.226	0.068	0.941	5.795	0.152	10.33	43.42

*OC calculated for major electronic contribution from HOMO to LUMO

SI Table 5 Simulated λ_{vert}, E_{vert}, f, LHE, τ_0 and % OC of SR1 to SR9 at TD-DFT/ωB97XD/6-311++G (d, p) level of theory

Dyes	λ_{vert} (nm)		E_{Vert} (eV)		*f*		LHE		τ_0 (sec)		% OC*	
	Vacuum	DMF	Vacuum	DMF	Vacuum	DMF	Vacuum	DMF	Vacuum	DMF	Vacuum	DMF
SR1	367.77	416.19	3.371	2.979	0.945	0.763	0.886	0.827	0.140	0.221	94.06	54.38
SR2	369.48	422.59	3.356	2.934	0.948	1.055	0.887	0.912	0.140	0.165	94.35	75.91
SR3	384.31	434.99	3.226	2.850	0.831	1.031	0.852	0.907	0.173	0.179	94.82	80.70
SR4	392.57	440.42	3.158	2.815	0.780	1.164	0.834	0.931	0.193	0.163	94.52	94.17
SR5	427.87	465.38	2.898	2.664	0.055	1.005	0.118	0.901	3.264	0.210	13.05	74.76
SR6	409.85	451.43	3.025	2.747	0.649	1.009	0.775	0.902	0.253	0.197	56.31	46.28
SR7	400.80	445.87	3.093	2.781	0.623	0.985	0.762	0.896	0.252	0.197	67.29	70.21
SR8	399.99	444.04	3.100	2.792	0.706	1.084	0.803	0.918	0.221	0.177	44.59	44.36
SR9	389.03	430.47	3.187	2.880	0.795	1.176	0.840	0.933	0.186	0.154	50.52	37.93

*OC calculated for major electronic contribution from HOMO to LUMO

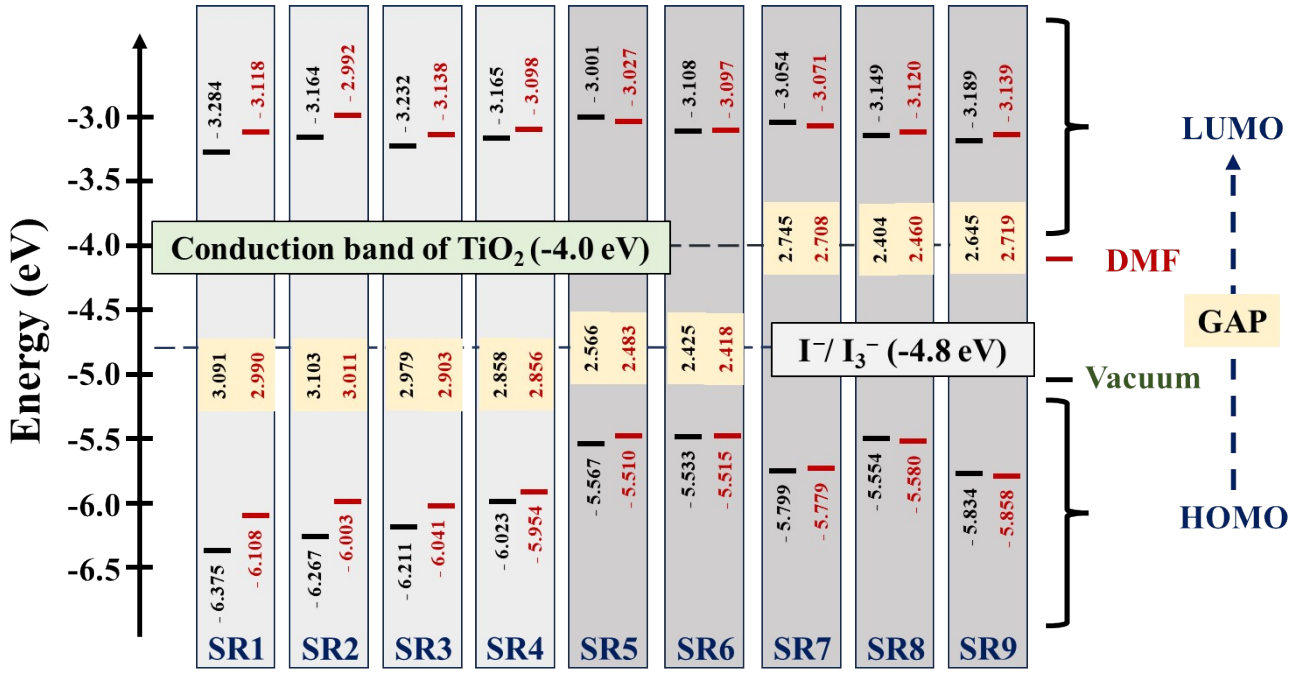

SI Fig. 1 Energies profile diagram of SR1 to SR9 optimized at B3LYP/6-311++G (d, p) level of theory

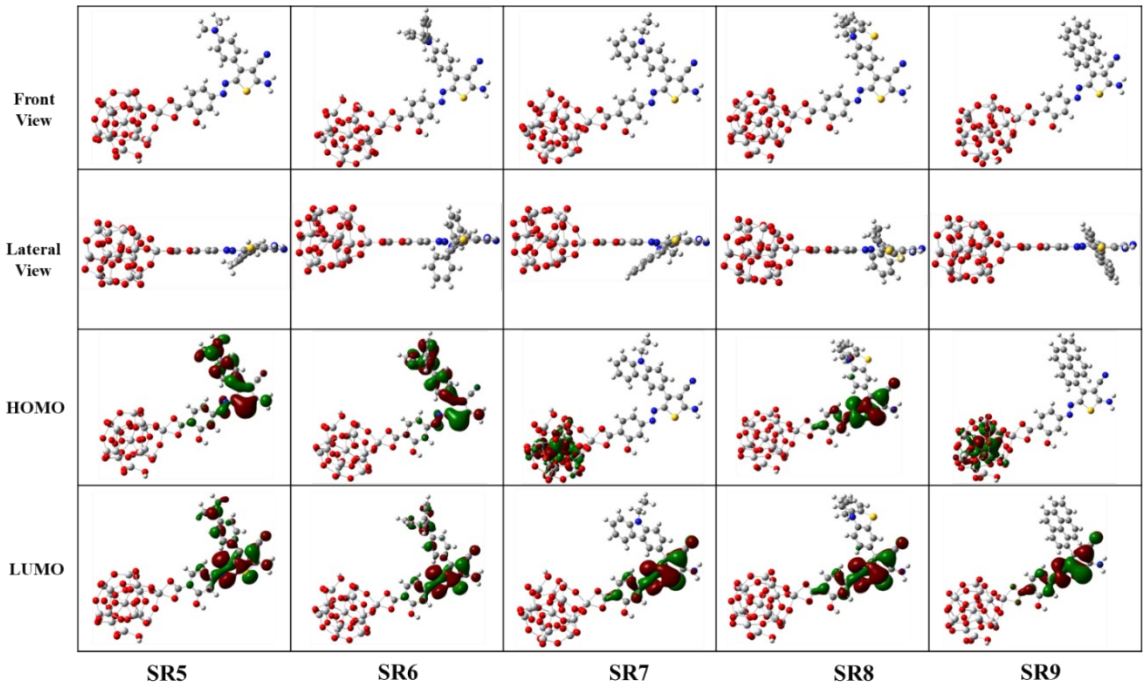

SI Fig. 2 Optimized geometries, HOMO, and LUMO diagram of SR5 to SR9 optimized at DFT/B3LYP/LANL2DZ/6-31G(d)

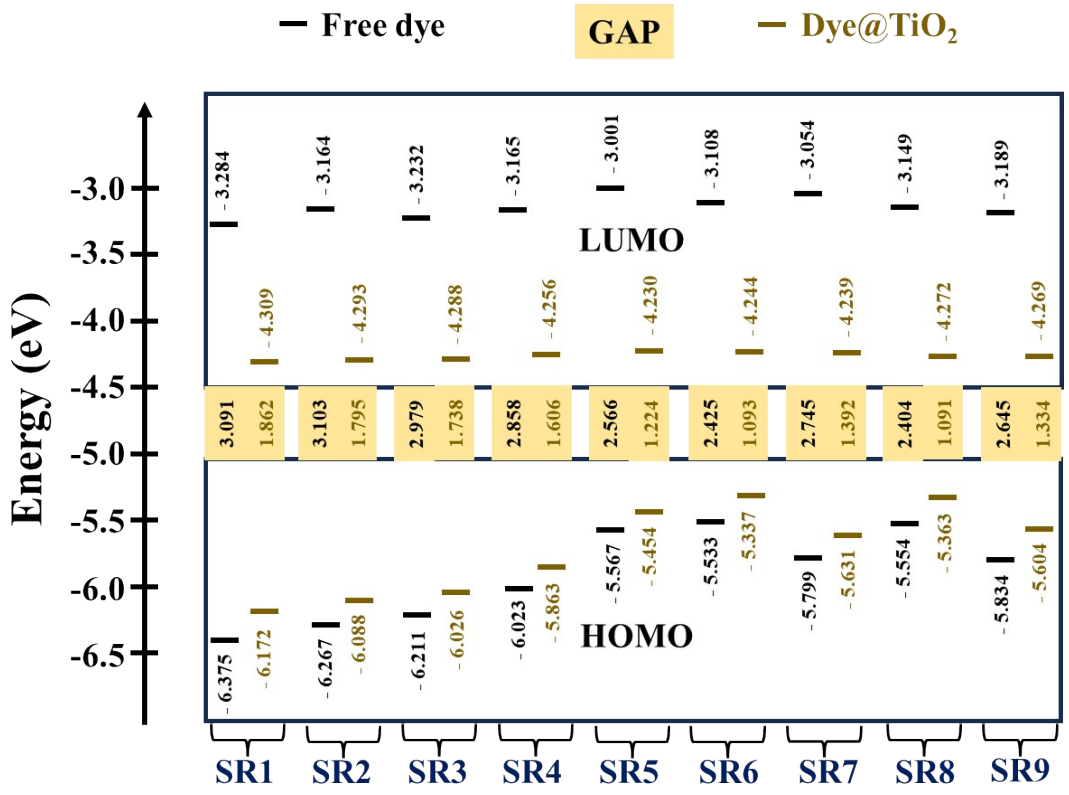

SI Fig. 3 A comparative HOMO-LUMO energy level diagram of SR1 to SR9 with and without TiO2 cluster optimized at B3LYP/6-311++G (d, p) and B3LYP/6-31G (d)/LANL2DZ

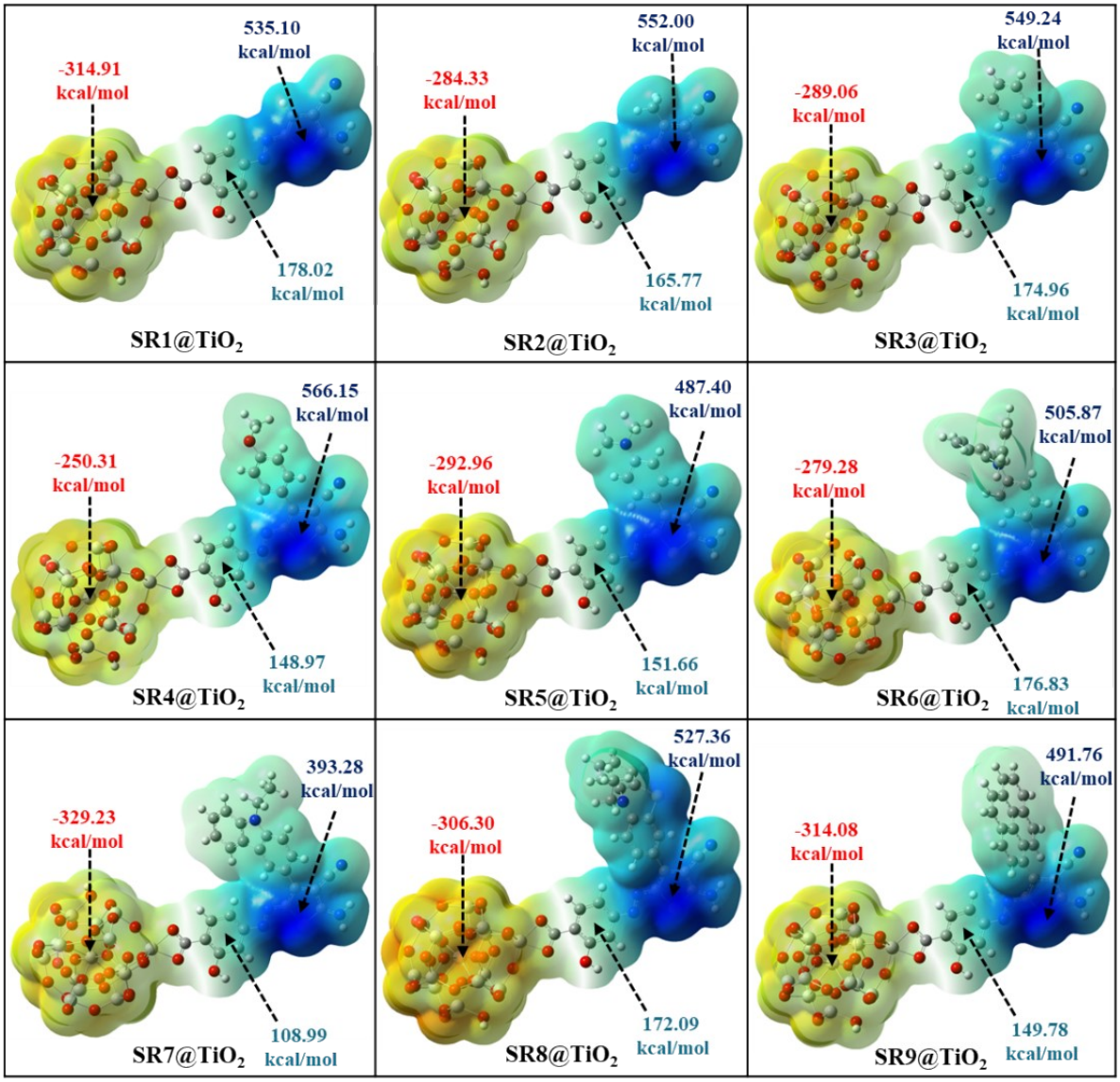

SI Fig. 4 MEP plots of SR1 to SR9 bound to TiO_2 at DFT/B3LYP/6-31G(d)/LANL2DZ level of theory

SI Table 6 Computed linear polarizability of AB1 to AB9 dyes

Dyes	Linear polarizability (α_0) × 10^{-24} esu					
	B3LYP		CAM-B3LYP		ωB97XD	
	Vacuum	DMF	Vacuum	DMF	Vacuum	DMF
SR1	38.90	55.97	36.53	51.43	36.34	51.09
SR2	40.78	58.80	38.48	54.41	38.31	54.11
SR3	49.72	71.89	47.08	66.82	46.88	66.51
SR4	53.56	76.90	53.56	71.25	50.32	70.88
SR5	58.84	86.10	55.06	78.45	54.69	77.81
SR6	77.80	110.42	72.47	101.14	71.99	100.50
SR7	67.91	98.34	64.09	91.11	63.76	90.64
SR8	71.53	102.30	67.10	94.36	66.76	93.93
SR9	70.88	103.73	67.15	96.75	66.85	96.36

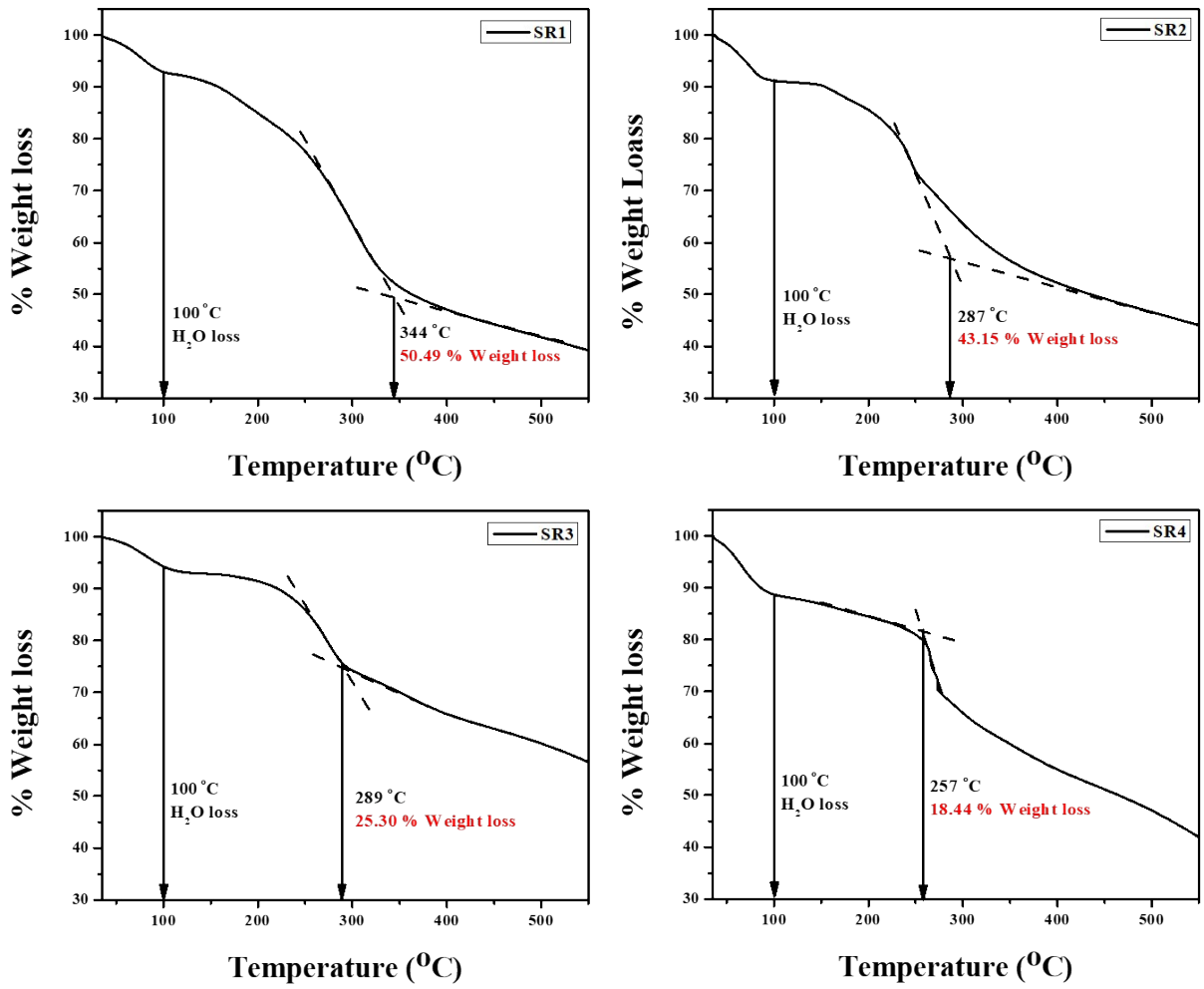

SI Fig. 5 TGA patterns of SR1 to SR4 dye

Materials and methods

2,5-dihydroxy-1,4-dithiane, 2,5-dimethyl-1,4-dithiane-2,5-diol (Sigma-Aldrich), 4-amino benzoic acid, acetophenone, 1-(4-methoxyphenyl)ethan-1-one, malononitrile, triethylamine, ammonium acetate (NH_4OAc), sodium nitrate ($NaNO_2$), sulfur (S_8), urea, glacial acetic acid (Gl. AcOH), concentrated hydrochloric acid (conc. HCl, 33%), sodium suphate (Na_2SO_4), n-hexane, toluene, ethyl acetate, methanol, and N, N-dimethylformamide (DMF) were bought from Spectrochem Chemicals Ltd, Mumbai, India. Solid and liquid solvents and reagents were used without any purification. TiO_2 nanopowder, ethyl cellulose, and α-terpineol were purchased from Sigma-Aldrich, India, and used without further purification. DN-ES104 electrolyte, which is an MNP-based electrolyte containing 3-methoxypropionitrile, 1-butyl-3-methylimidazolium iodide, guanidinium thiocyanate, iodine, and 1-butyl-1H-benzol[d]imidazole was purchased from "dynamo." Solvents used for cyclic voltammetry (CV) were purified using a standard protocol and stored under 4A molecular sieves.

"Perkin Elmer spectrophotometer" with 1 cm quartz cells was used to record UV visible absorption spectra of the titled dyes. The dyes of 15 μM are taken for UV visible study. The progress of reactions is observed by the Thin-layer chromatography (TLC) technique (60 F254) Merck, India. The recrystallization and column chromatography techniques were used to attain the purification of all compounds. The FT-IR bands of the synthesized dyes are recorded on the Bruker ALPHA-II instrument. "Agilent 400 and 500 MHz" with tetramethylsilane (TMS) as the internal standard was used to record the synthesized dyes' ^{1}H NMR and ^{13}C NMR spectra, respectively. The DMSO-d6 solvent was used for sample preparation. "Shimadzu Lab solution instrument" with averaged ESI positive+ was used to analyze the mass of titled dyes. Cyclic voltammetry (CV) was performed in Metrohm Autolab electrochemical analyzer following a three-electrode system where a glassy carbon electrode acts as working, Pt-wire as counter, and Ag/Ag+ as reference electrode in DMF at 25 mV/sec scan rate. A supporting electrolyte was added 0.1 M TBAPF6, and the electrode was externally calibrated with ferrocene. Thermogravimetric analysis was carried out using the STA7300/Hitachi instrument. Most importantly, cell fabrication was carried out using Elixir technologies DSSC fabrication setup.

Fabrication of Cell

The FTO (Fluorine Doped Tin Oxide) coated glass substrate was first treated with surfactant, distilled water, and alcohol before the doctor blading from titania paste made of nanocrystalline TiO2 and additives. The TiO_2-coated electrode was slowly heated in the muffle furnace at 500 °C. The resulting TiO_2 thickness is approximately 12 μm. The TiO_2 was then deep for 20 hours at room temperature without exposure to light in a dye solution of sensitizer prepared by dissolving 30mg of dye sample into the solvent mixture of 60 ml of ethanol and 20 ml of acetonitrile. The counter electrode (Pt) was prepared through a screen printing technique on an FTO glass surface. The Pt-coated electrode was then heated slowly up to 500 °C. After cooling to room temperature, two holes were drilled to inject the electrolyte through them. The device was made by sandwiching these two opposing electrodes with a UV sealant. The cell was made harder by exposing it to UV light for 2 minutes. Later, the DN-ES104 electrolyte was injected into the cell through holes previously bored in the Pt-counter electrode. After that, both the holes were sealed with UV sealant and made harder by exposing the cell to UV light for 2 minutes. Before the photovoltaic test, all DSSC devices were kept in a dark area for 24 hours. The devices' active area is approximately 1.0 cm^2, and in order to reduce the effect of stray light during measurement, a black mask was employed as the aperture.[6]

Synthesis of couplers 2-aminothiophene-3-carbonitrile (C1) and 2-amino-4-methylthiophene-3-carbonitrile (C2): Couplers C1 and C2 were synthesized with the reported method described by Zita et al. [7] **with some minor modification as discussed below.**

2-aminothiophene-3-carbonitrile (C1) [7]: compound 2,5-dihydroxy-1,4-dithiane (S1) (1 equivalent, 0.066 mol, 10g) and malononitrile (2 equivalent, 0.131 mol, 8.67 g) were dissolved or mixed in methanol (20 mL). The resultant solution was allowed to cool around 10 °C. After cooling, triethylamine (1 equivalent, 0.066 mol, 7.16 mL) was slowly added to the stirred solution so that the reaction mixture's temperature would not rise drastically. After adding triethylamine, the reaction mixture was subjected to reflux between 60-70 °C. After completion of the reaction (usually takes 2-3 h), which was monitored through TLC, the reaction mixture was cooled and poured into the ice-cold water. The resultant precipitate was filtered and recrystallized with n-hexane to yield 7.6 g (93.14 %, M.p. = 102-104 °C) of pure pale-brown colored solid of C1.

2-amino-4-methylthiophene-3-carbonitrile (C2): compound 2,5-dimethyl-1,4-dithiane-2,5-diol (S2) (1 equivalent, 0.055 mol, 10g) and malononitrile (2 equivalent, 0.111 mol, 7.33 g) were dissolved or mixed in methanol (20 mL). The resultant solution was allowed to cool around 10 °C. After cooling, triethylamine (1 equivalent, 0.055 mol, 7.73 mL) was slowly added to the stirred solution so that the reaction mixture's temperature would not rise drastically. After adding triethylamine, the reaction mixture was subjected to reflux between 60-70 °C. After completion of the reaction (usually takes 2-3 h), which was monitored through TLC, the reaction mixture was cooled and poured into the ice-cold water. The resultant precipitate was filtered and recrystallized with n-hexane to yield 6.95 g (90.67 %, M.p. = 116 - 118 °C) of pure off-white colored solid of C2.

Synthesis of 2-(1-phenylethylidene)malononitrile (S5), 2-(1-(4-methoxyphenyl)ethylidene)malononitrile (S6) and couplers 2-amino-4-phenylthiophene-3-carbonitrile (C3) and 2-amino-4-(4-methoxyphenyl)thiophene-3-carbonitrile (C4)

Compounds S5 and S6 are synthesized as per the reported method given by Mogens et al. [8] **with some modifications.**

2-(1-phenylethylidene)malononitrile (S5) [8]: Acetophenone (S3) (1 equivalent, 18.5 g, 0.154 mmol), malononitrile (2.8 equivalent, 28.4 g,0.430 mmol), NH_4OAc (3.37 equivalent, 40 g, 0.519 mmol), and AcOH (6.5 equivalent, 60 mL, 1 mol) are mixed in toluene (500 mL). The flask was equipped with a Dean-Stark apparatus, and the reaction mixture was refluxed at 180 °C for 3 h. After cooling the reaction mixture, the reaction mixture was diluted with ethyl acetate and, washed with water, brine, and dried with Na_2SO_4. Further evaporating the solvent and recrystallizing the crude brown solid with boiling heptane gave S5 (22.17 g, 85.61 %) as pale yellow crystals. Mp. 93.0 – 95.0 °C.

2-(1-(4-methoxyphenyl)ethylidene)malononitrile (S6): 1-(4-methoxyphenyl)ethan-1-one (S4) (1 equivalent, 20.71 g, 0.138 mmol), malononitrile (2.8 equivalent, 25.50 g,0.386 mmol), NH_4OAc (3.37 equivalent, 35.82 g, 0.465 mmol), and AcOH (6.5 equivalent, 52 mL, 0.896 mol) are mixed in toluene (500 mL). The flask was equipped with a Dean-Stark apparatus, and the reaction mixture was refluxed at 180 °C for 3 h. After cooling the reaction mixture, the reaction mixture was diluted with ethyl acetate and, washed with water, brine, and dried with Na_2SO_4. Further evaporating the solvent and recrystallizing the crude brown solid with boiling heptane gave S5 (19.55 g, 71.53 %) as pale yellow crystals. Mp. 87.0 – 89.0 °C.

Couplers 2-(1-phenylethylidene)malononitrile (C3) and 2-amino-4-(4-methoxyphenyl)thiophene-3-carbonitrile (C4) were synthesized as per methods reported by Wardakhan et al. [9] with some modification.

2-amino-4-phenylthiophene-3-carbonitrile (C3) and 2-amino-4-(4-methoxyphenyl)thiophene-3-carbonitrile (C4) [9]**:** 2-(1-phenylethylidene)malononitrile (S5) (1 equivalent, 1.68 g, 0.01 mol), or 2-(1-(4-methoxyphenyl)ethylidene)malononitrile (S6) (1 equivalent, 1.98 g, 0.01 mol) and sulfur (1 equivalent, 0.32 g, 0.01 mol) in absolute ethanol (50 mL) containing triethylamine (0.5 mL) were heated under reflux for 2-3 h. After the reaction (confirming through TLC) was completed, the reaction mixture was poured into iced water, and the resultant precipitate was then recrystallized with absolute ethyl alcohol to yield 1.60g (80.0 %) of C3 and 1.06g (91.22%) of C4.

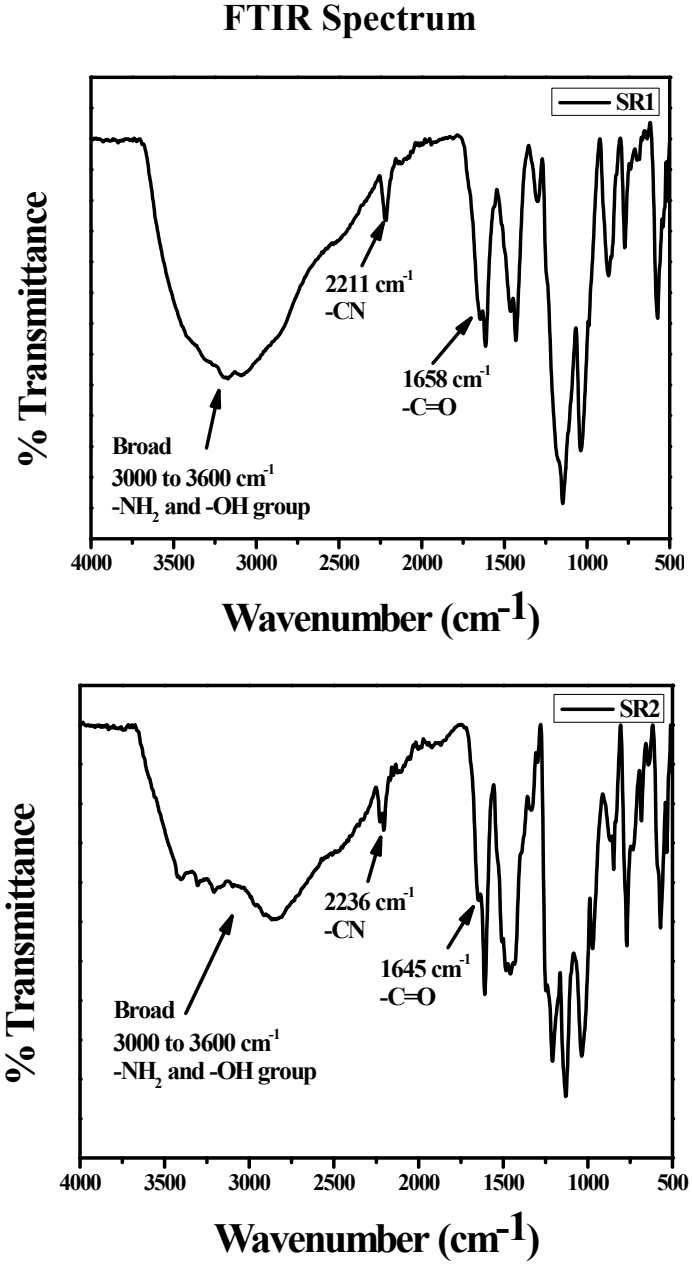

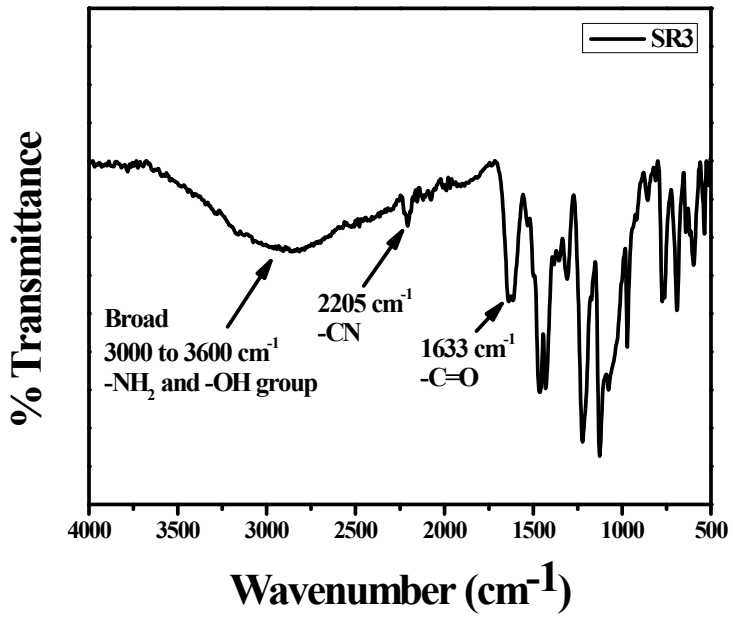
SR3
% Transmittance
Broad
3000 to 3600 cm-1
-NH2 and -OH group
2205 cm-1
-CN
1633 cm-1
-C=O
4000
3500
3000
2500
2000
1500
1000
500
Wavenumber (cm-1)

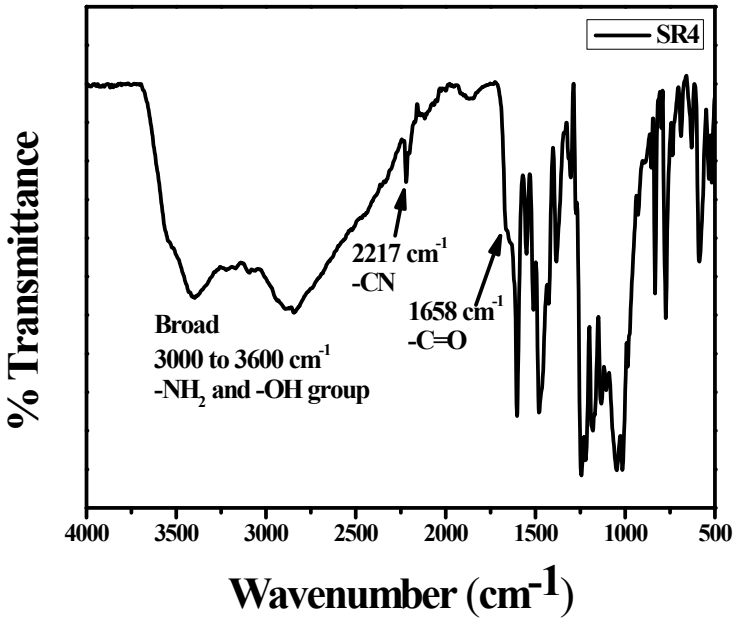
SR4
% Transmittance
Broad
3000 to 3600 cm-1
-NH2 and -OH group
2217 cm-1
-CN
1658 cm-1
-C=O
4000
3500
3000
2500
2000
1500
1000
500
Wavenumber (cm-1)

^{1}H NMR Spectrum

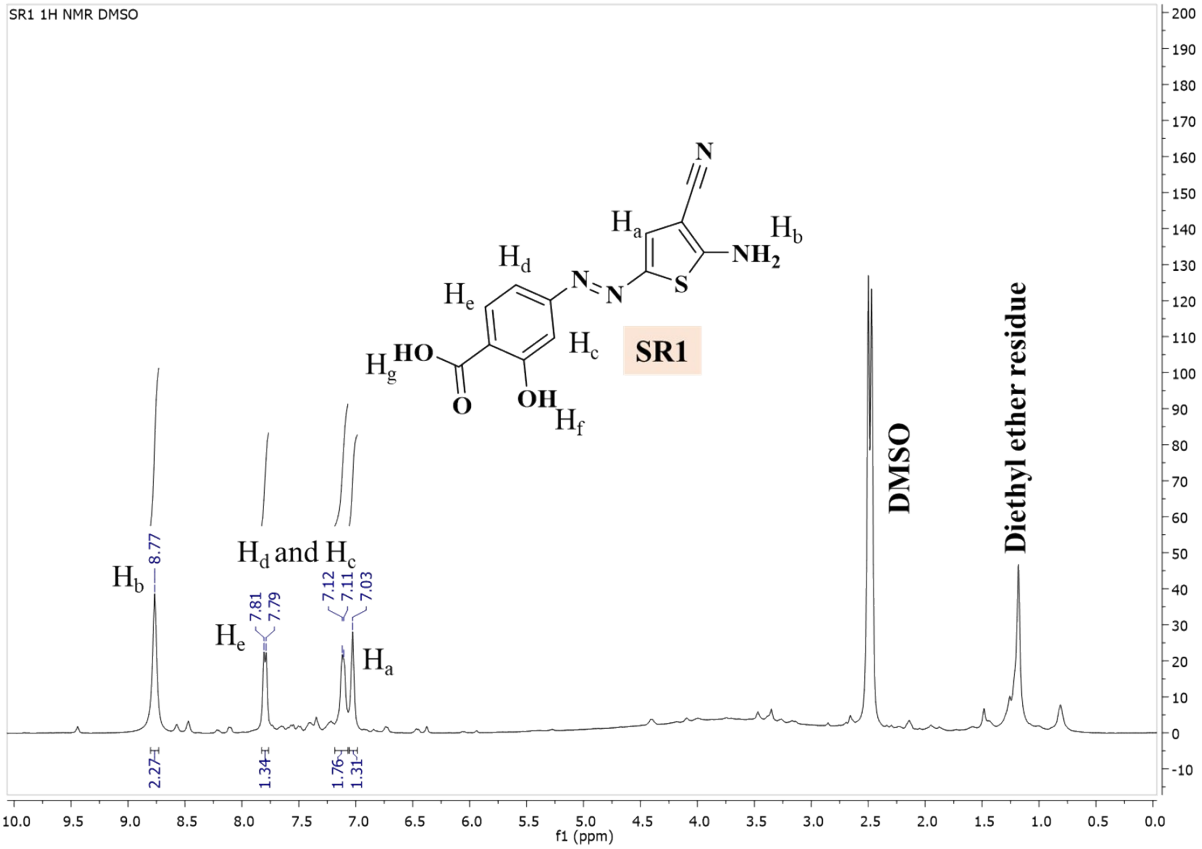

^{1}H NMR (400 MHz, DMSO-d^{6}) δ (H_b) 8.77 (s, 2H), (H_e) 7.80 (d, *J* = 7.3 Hz, 1H), (H_c and H_d) 7.11 (d, *J* = 5.4 Hz, 2H), (Há) 7.03 (s, 1H).

Peak names	δ (ppm)	Signal
H_a	7.03	s, 1H
H_b	8.77	s, 2H
H_c	7.11	d, *J* = 5.4 Hz, 2H
H_d		
H_e	7.80	d, *J* = 7.3 Hz, 1H

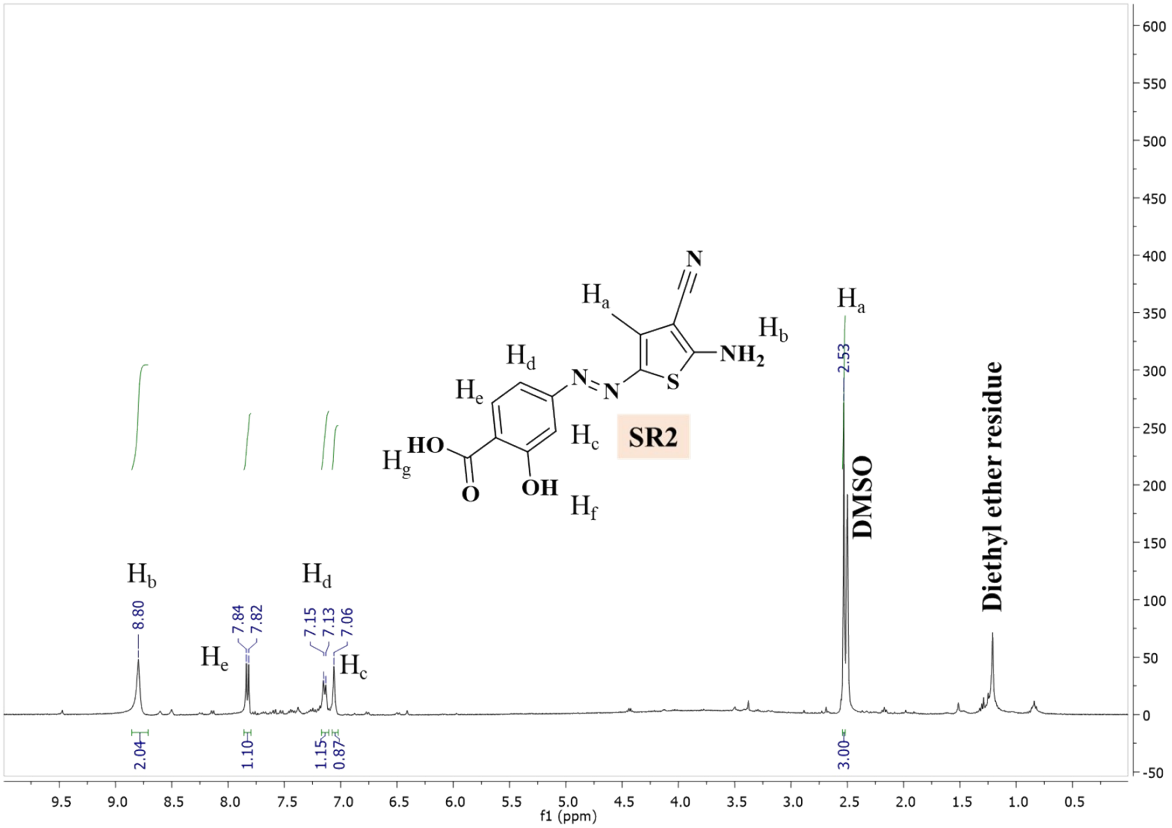

^{1}H NMR (400 MHz, DMSO-d^{6}) δ (H_b) 8.80 (s, 2H), (H_e) 7.83 (d, J = 8.4 Hz, 1H), (H_d) 7.14 (d, J = 8.1 Hz, 1H), (H_c) 7.06 (s, 1H), (H_a) 2.53 (s, 3H).

Peak names	δ (ppm)	Signal
H_a	2.53	s, 3H
H_b	8.80	s, 2H
H_c	7.06	s, 1H
H_d	7.14	d, J = 8.1 Hz, 1H
H_e	7.83	d, J = 8.4 Hz, 1H

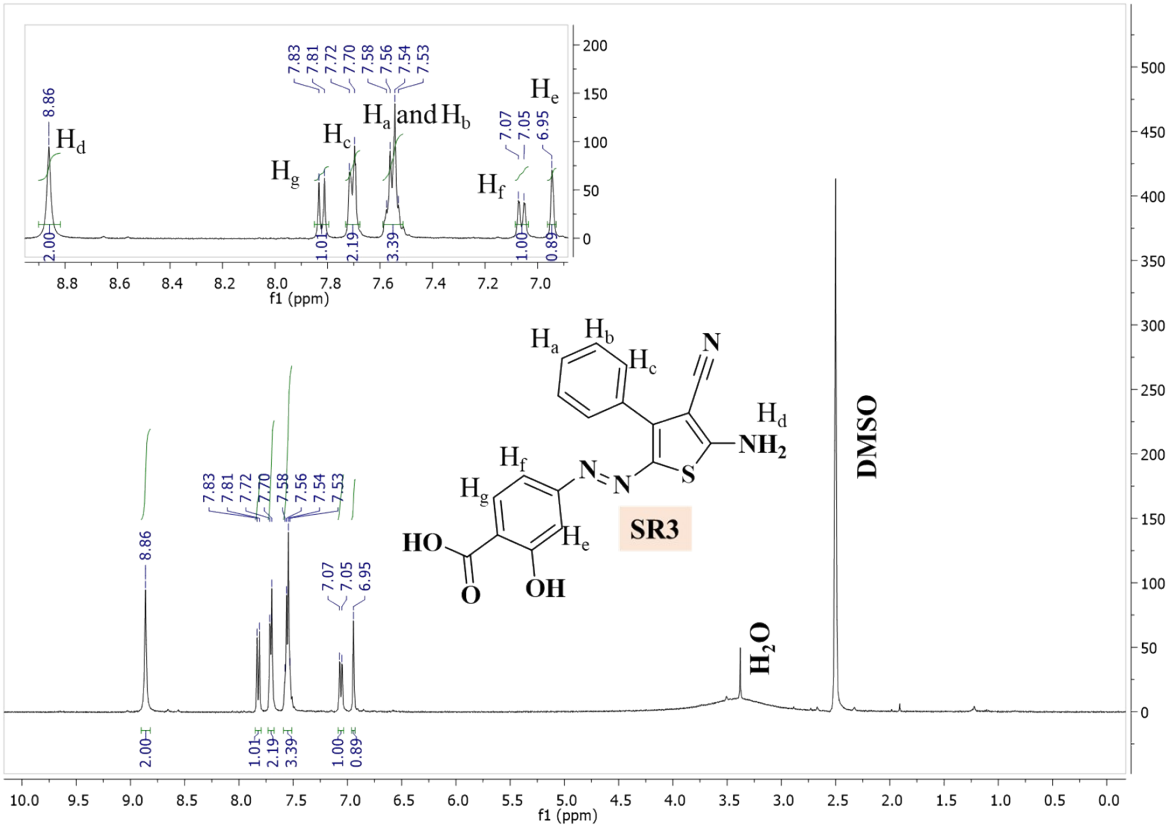

^{1}H NMR (400 MHz, DMSO-d^{6}) δ (H_d) 8.86 (s, 2H), (H_g) 7.82 (d, J = 8.5 Hz, 1H), (H_c) 7.71 (d, J = 8.0 Hz, 2H), (H_a and H_b) 7.55 (m, J = 5.4 Hz, 3H), (H_f) 7.06 (d, J = 8.4 Hz, 1H), (H_e) 6.95 (s, 1H).

Peak names	δ (ppm)	Signal
H_a	7.55	m, J = 5.4 Hz, 3H
H_b		
H_c	7.71	d, J = 8.0 Hz, 2H
H_d	8.86	s, 2H
H_e	6.95	s, 1H
H_f	7.06	d, J = 8.4 Hz, 1H
H_g	7.82	d, J = 8.5 Hz, 1H

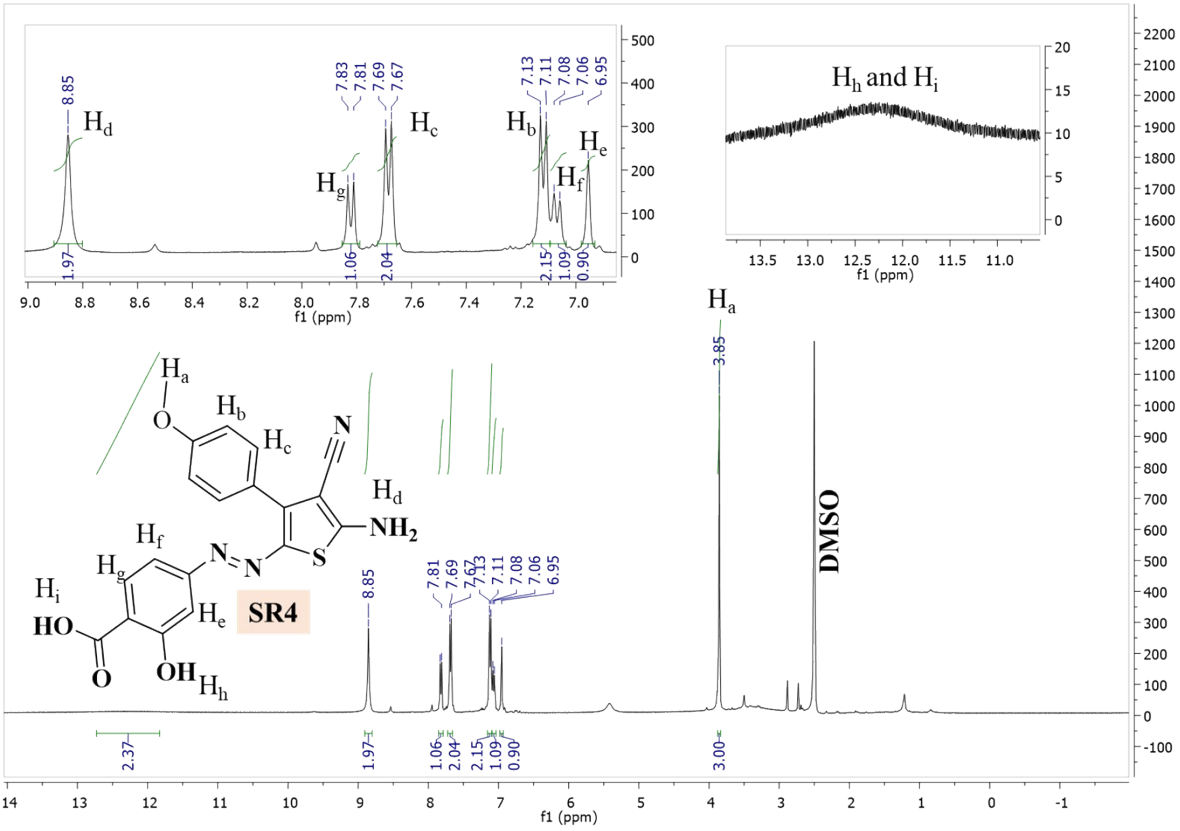

1H NMR (400 MHz, DMSO-d^6) δ (H_h and H_i) 11.0 to 13.5 (Broad s, 2H), (H_d) 8.85 (s, 2H), (H_g) 7.82 (d, J = 8.5 Hz, 1H), (H_c) 7.68 (d, J = 8.5 Hz, 2H), (H_b) 7.12 (d, J = 8.5 Hz, 2H), (H_f) 7.07 (d, J = 8.5 Hz, 1H), (H_e) 6.95 (s, 1H), (H_a) 3.85 (s, 3H).

Peak names	δ (ppm)	Signal
H_a	3.85	s, 3H
H_b	7.12	d, J = 8.5 Hz, 2H
H_c	7.68	d, J = 8.5 Hz, 2H
H_d	8.85	s, 2H
H_e	6.95	s, 1H
H_f	7.07	d, J = 8.5 Hz, 1H
H_g	7.82	d, J = 8.5 Hz, 1H
H_h	Weak broad singlet 11.0 to 13.5	Broad s, 2H
H_i		

^{13}C NMR Spectrum

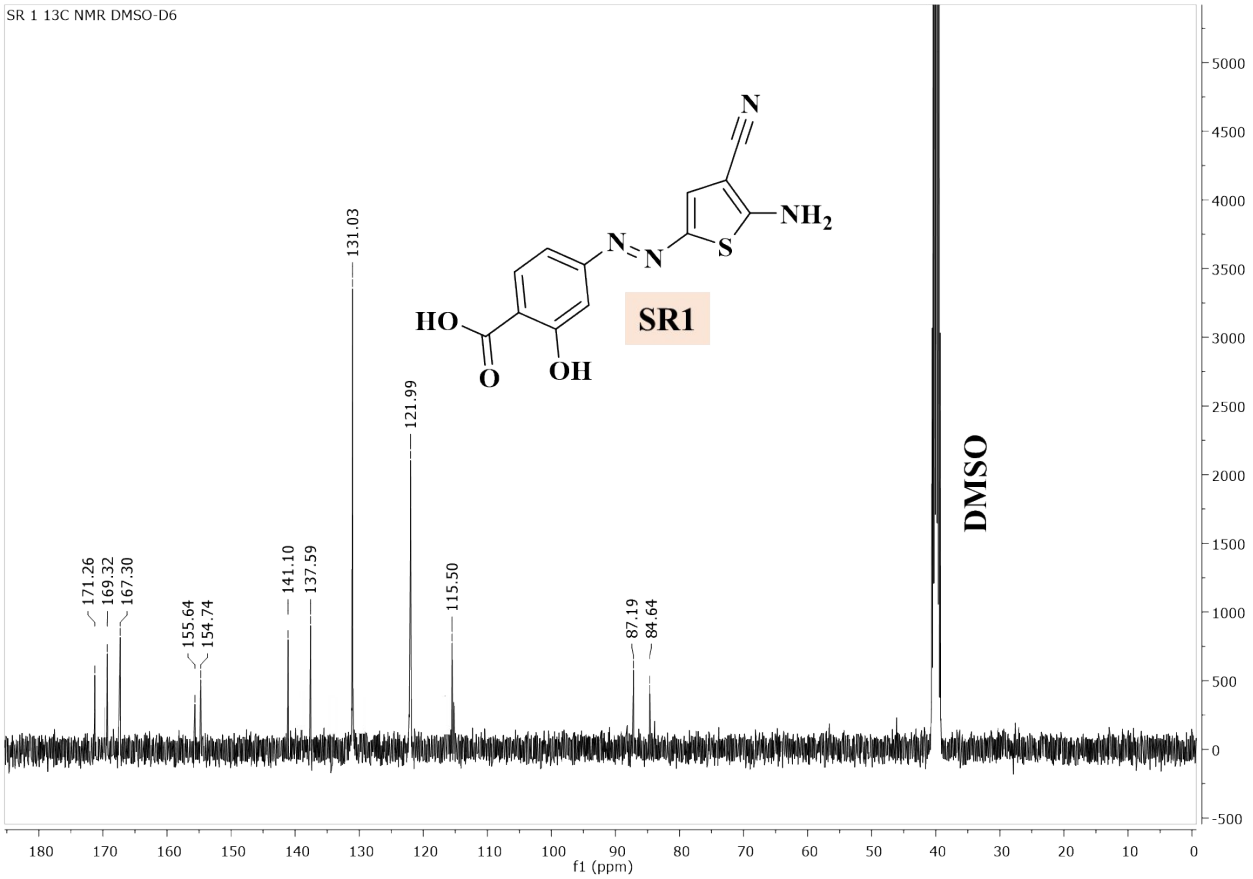

^{13}C NMR (101 MHz, DMSO-d^{6}) δ 171.26, 169.32, 167.30, 155.64, 154.74, 141.10, 137.59, 131.03, 121.99, 115.50, 87.19, 84.64.

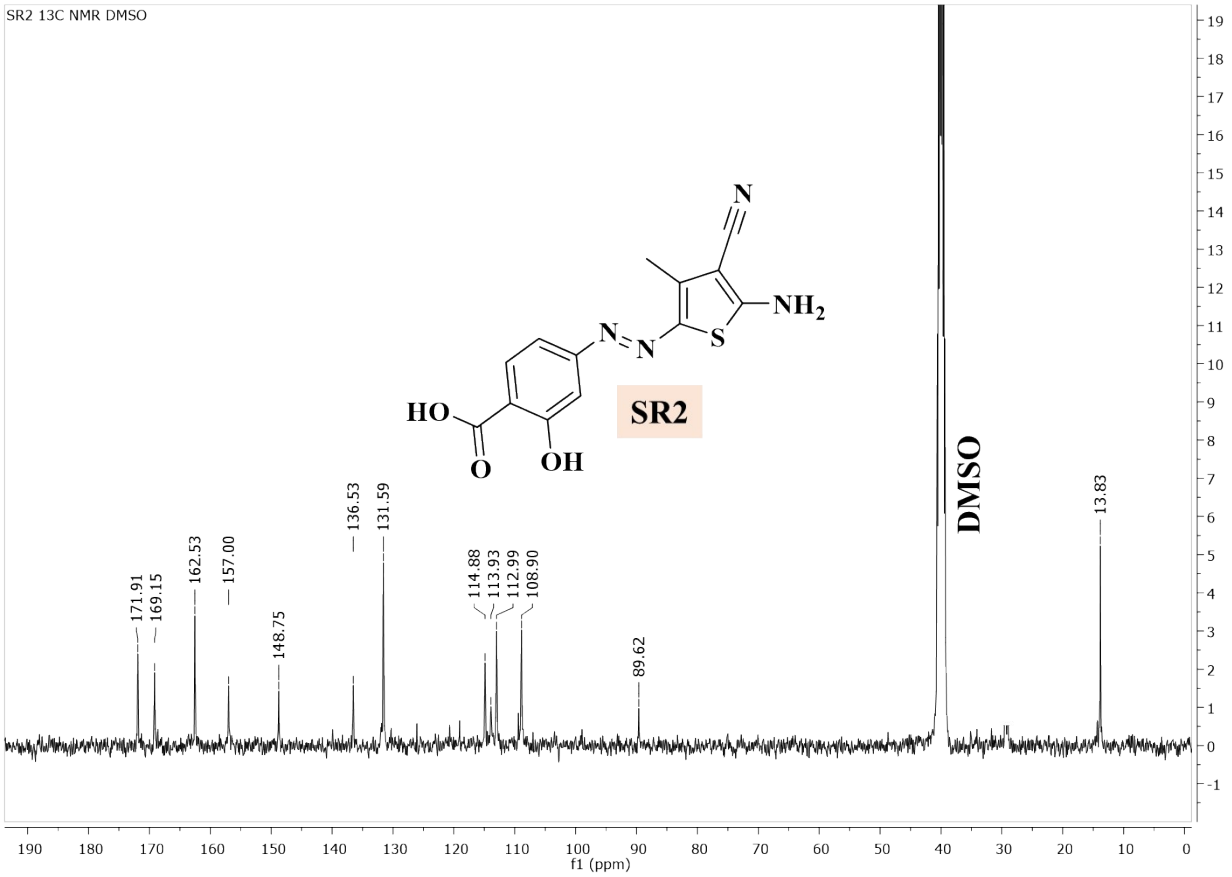

^{13}C NMR (101 MHz, DMSO-d^{6}) δ 171.91, 169.15, 162.53, 157.00, 148.75, 136.53, 131.59, 114.88, 113.93, 112.99, 108.90, 89.62, 13.83.

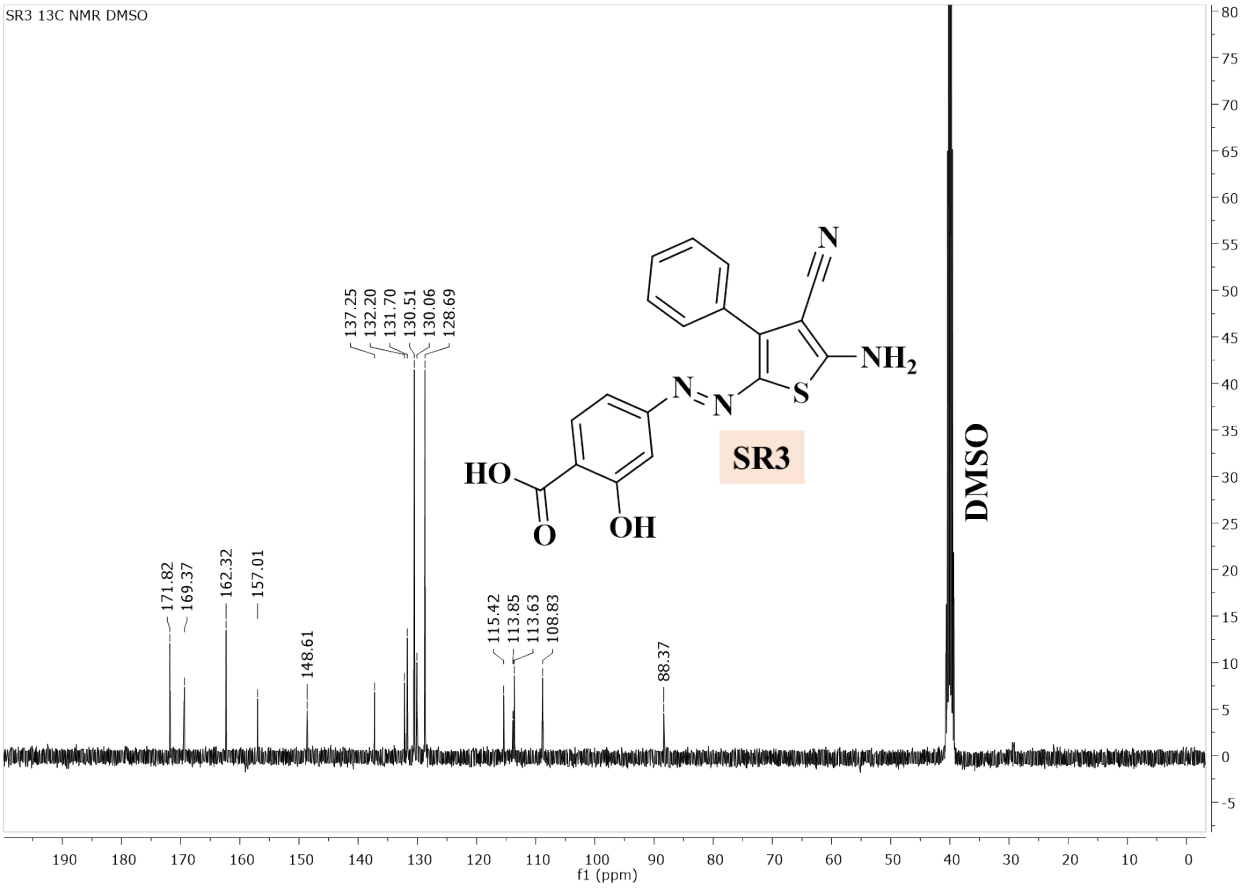

^{13}C NMR (101 MHz, DMSO-d^{6}) δ 171.82, 169.37, 162.32, 157.01, 148.61, 137.25, 132.20, 131.70, 130.51, 130.06, 128.69, 115.42, 113.85, 113.63, 108.83, 88.37.

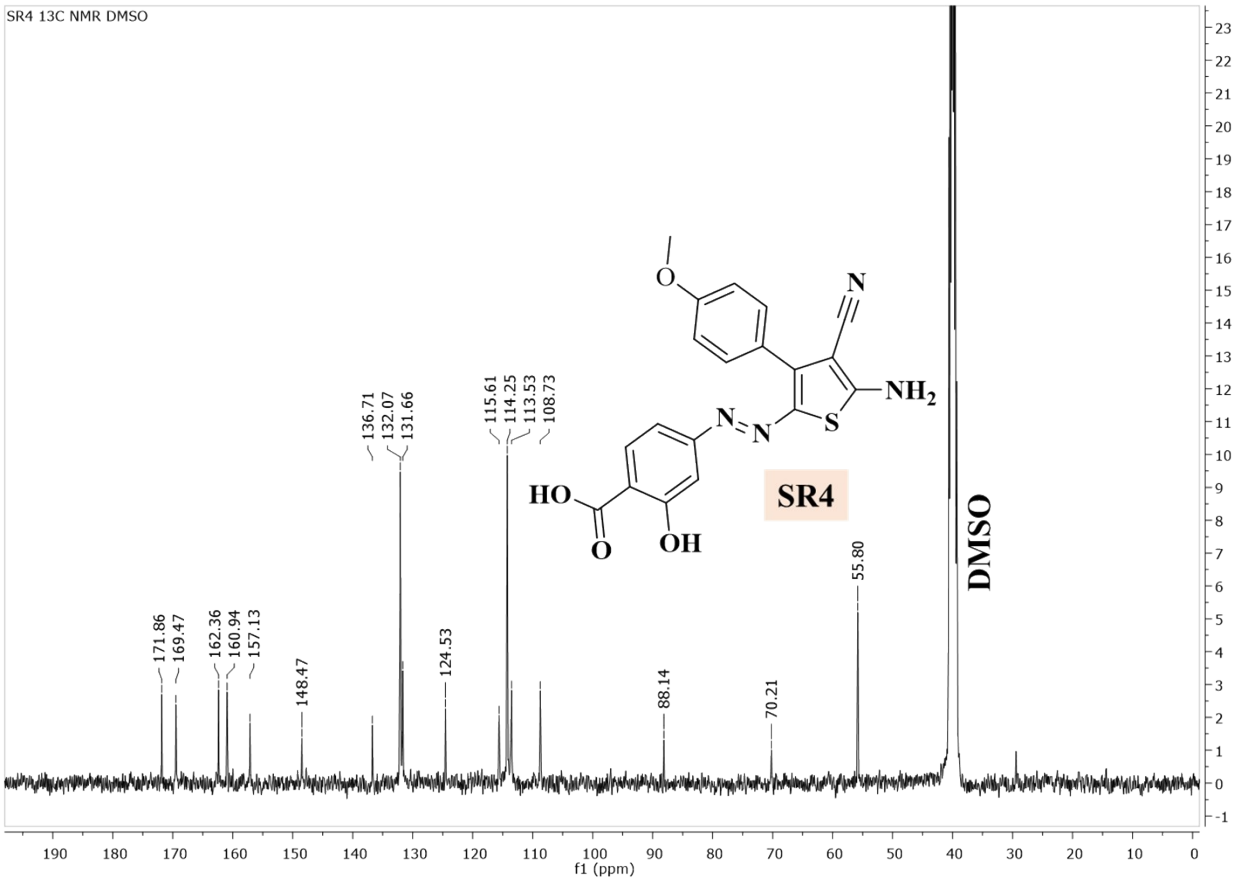

^{13}C NMR (101 MHz, DMSO-d^{6}) δ 171.86, 169.47, 162.36, 160.94, 157.13, 148.47, 136.71, 132.07, 131.66, 124.53, 115.61, 114.25, 113.89, 108.73, 88.14, 70.21, 55.80.

HRMS spectrum

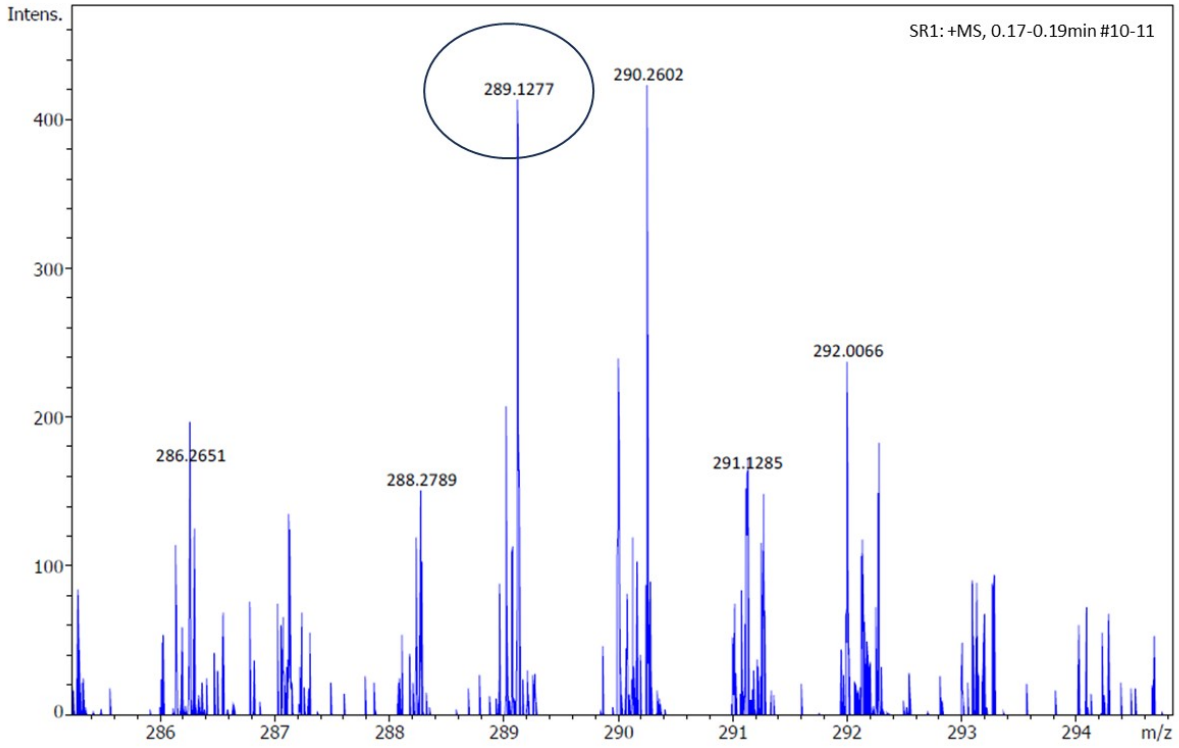

SR1 MS (m/z): calculated 288.03, for $C_{12}H_8N_4O_3S$ [M+H] + found 289.12

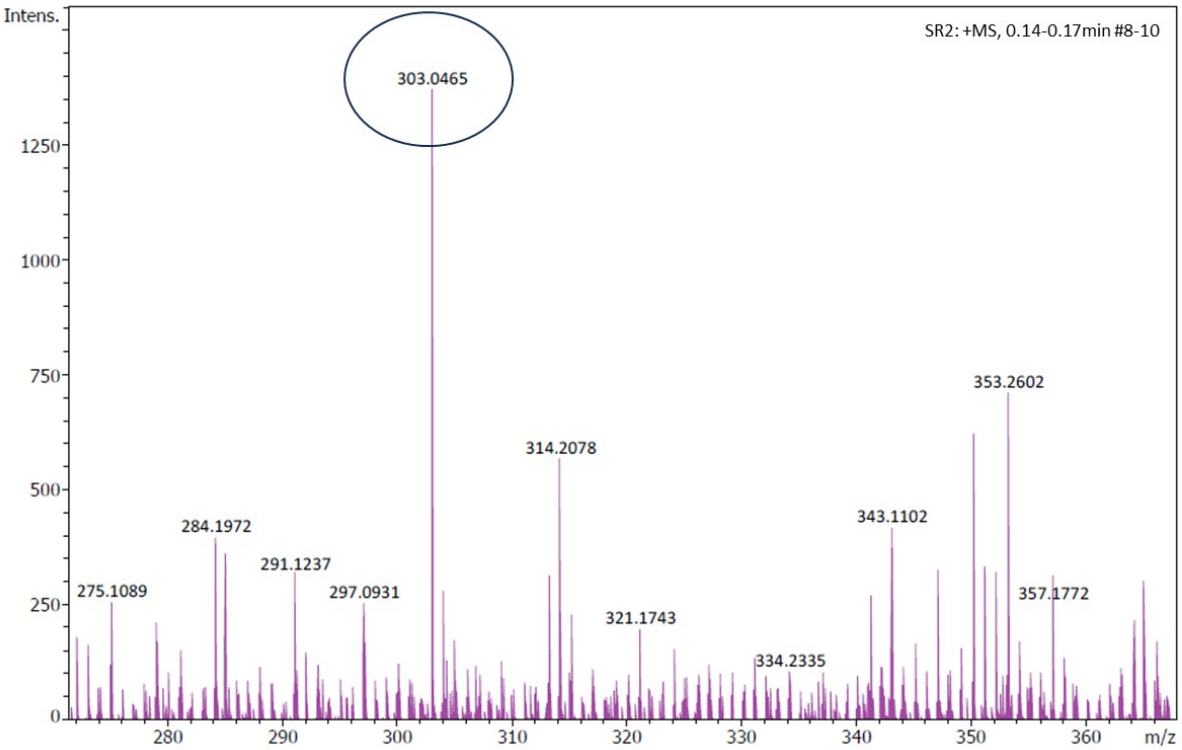

SR2 MS (m/z): calculated 302.05, for $C_{13}H_{10}N_4O_3S$ [M+H] + found 303.04

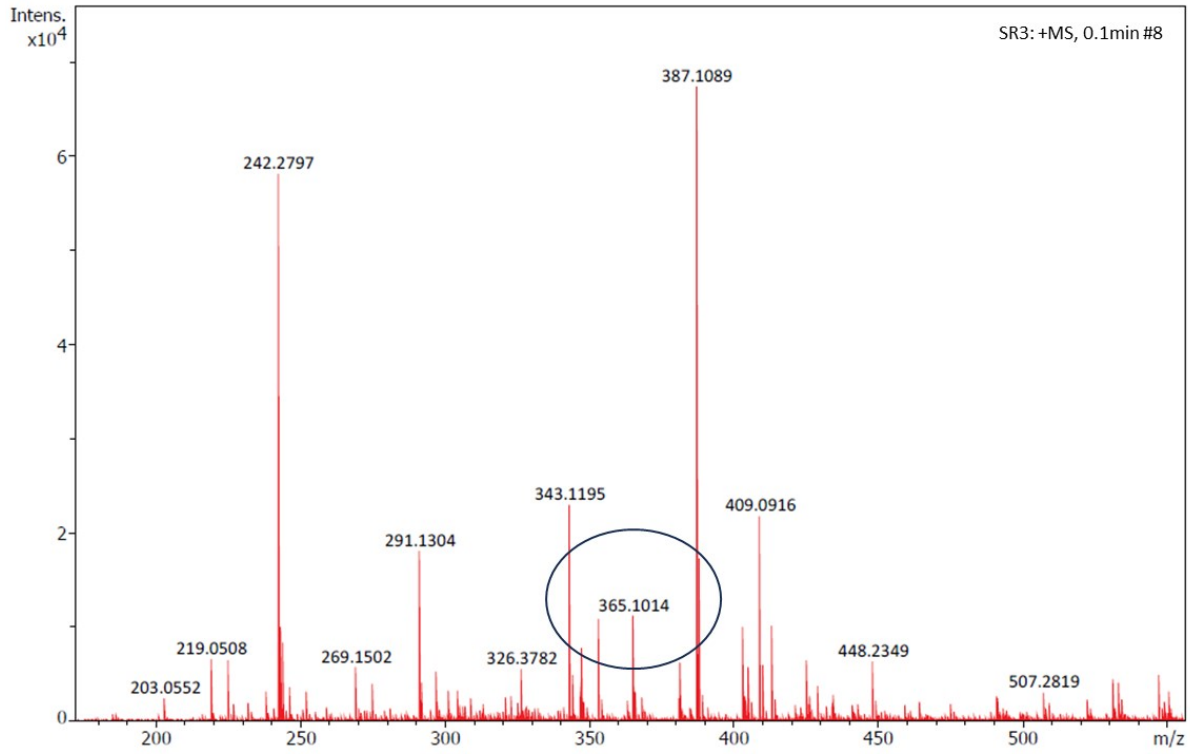

SR3 MS (m/z): calculated 364.06, for $C_{18}H_{12}N_4O_3S$ [M+H] + found 365.10

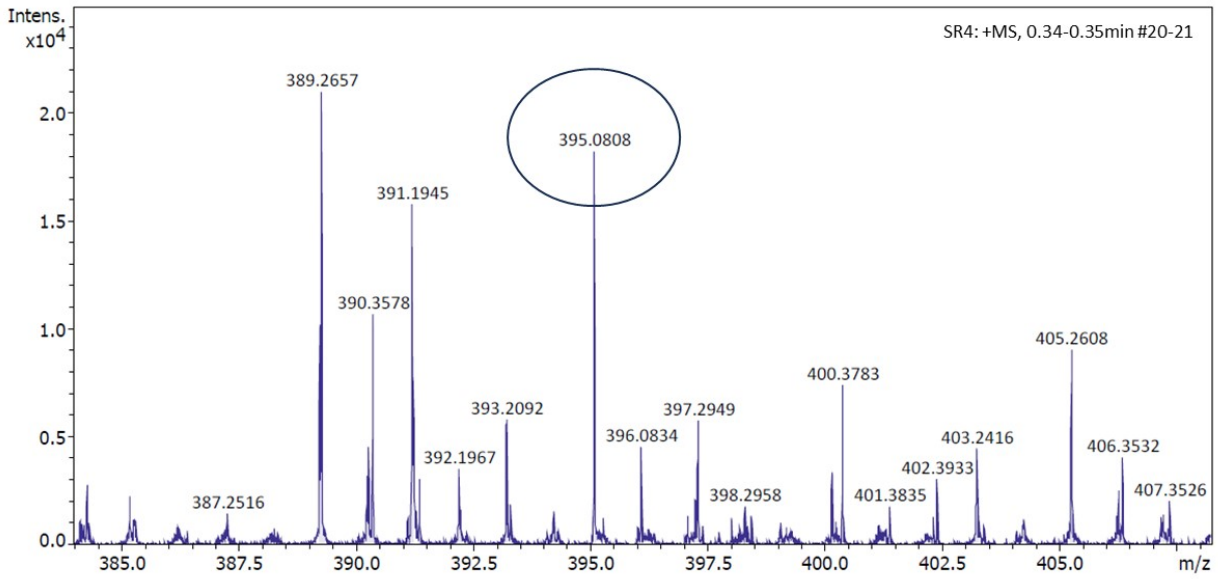

SR4 MS (m/z): calculated 394.07, for $C_{19}H_{14}N_4O_4S$ [M+H] + found 395.08

DOS Spectrum of title dyes and dyes@TiO_2

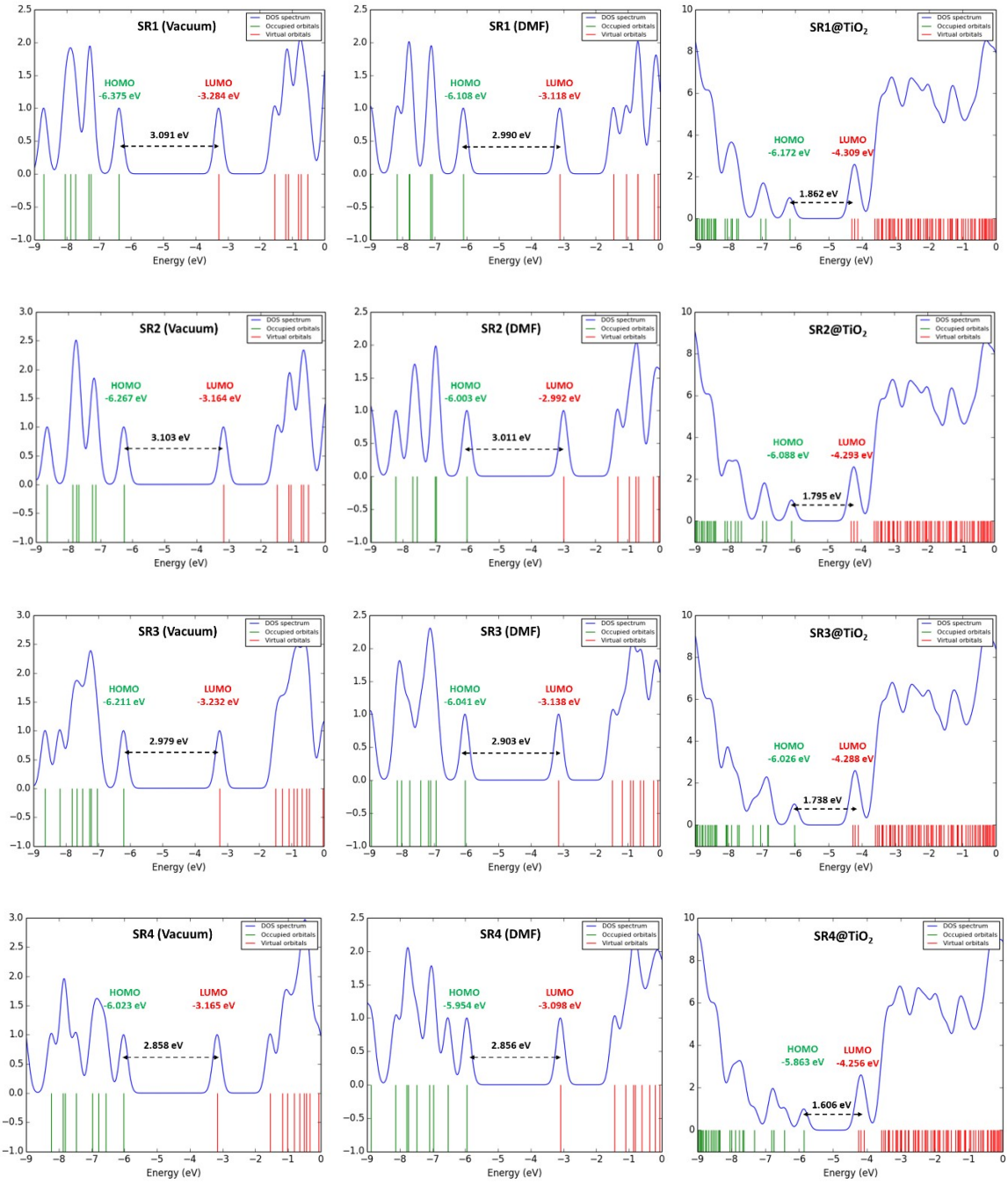

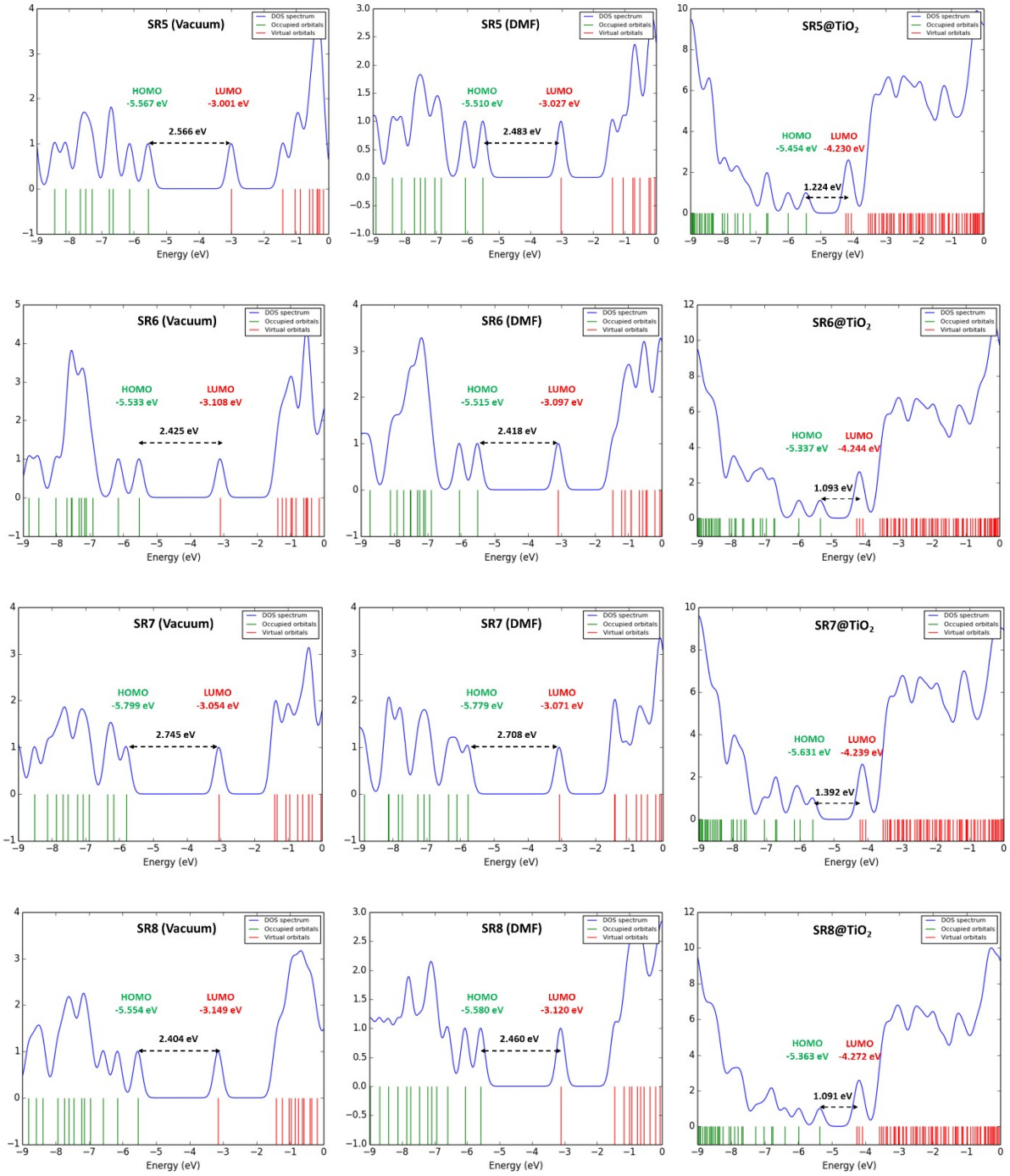
SR5 (Vacuum)
HOMO -5.567 eV
LUMO -3.001 eV
2.566 eV
SR5 (DMF)
HOMO -5.510 eV
LUMO -3.027 eV
2.483 eV
SR5@TiO2
HOMO -5.454 eV
LUMO -4.230 eV
1.224 eV
SR6 (Vacuum)
HOMO -5.533 eV
LUMO -3.108 eV
2.425 eV
SR6 (DMF)
HOMO -5.515 eV
LUMO -3.097 eV
2.418 eV
SR6@TiO2
HOMO -5.337 eV
LUMO -4.244 eV
1.093 eV
SR7 (Vacuum)
HOMO -5.799 eV
LUMO -3.054 eV
2.745 eV
SR7 (DMF)
HOMO -5.779 eV
LUMO -3.071 eV
2.708 eV
SR7@TiO2
HOMO -5.631 eV
LUMO -4.239 eV
1.392 eV
SR8 (Vacuum)
HOMO -5.554 eV
LUMO -3.149 eV
2.404 eV
SR8 (DMF)
HOMO -5.580 eV
LUMO -3.120 eV
2.460 eV
SR8@TiO2
HOMO -5.363 eV
LUMO -4.272 eV
1.091 eV
DOS spectrum
Occupied orbitals
Virtual orbitals
Energy (eV)

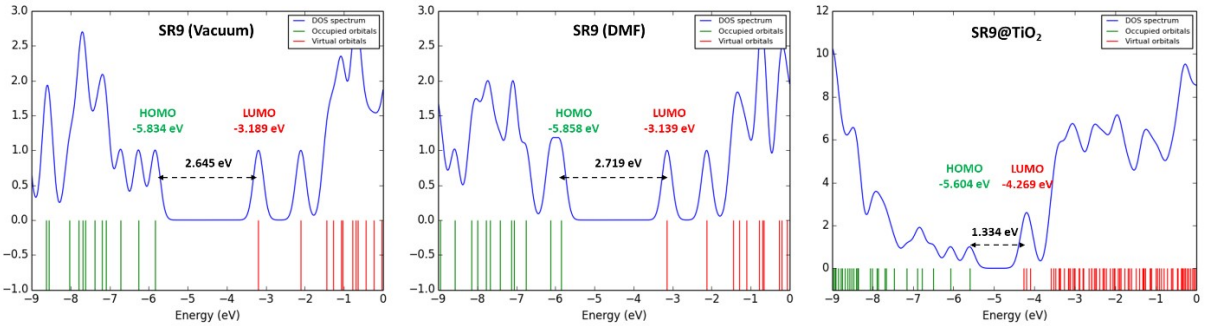

References

1 M. Grätzel, Recent Advances in Sensitized Mesoscopic Solar, *Acc. Chem. Res.*, 2009, **42**, 1788–1798.

2 A. Slimi, M. Hachi, A. Fitri, A. T. Benjelloun, S. Elkhattabi, M. Benzakour, M. Mcharfi, M. Khenfouch, I. Zorkani and M. Bouachrine, Effects of electron acceptor groups on triphenylamine-based dyes for dye-sensitized solar cells: Theoretical investigation, *J. Photochem. Photobiol. A Chem.*, , DOI:10.1016/j.jphotochem.2020.112572.

3 W. Sang-aroon, S. Saekow and V. Amornkitbamrung, Density functional theory study on the electronic structure of Monascus dyes as photosensitizer for dye-sensitized solar cells, *"Journal Photochem. Photobiol. A Chem.*, 2012, **236**, 35–40.

4 J. Zhang, Y. Kan, H. Li, Y. Geng, Y. Wu and Z. Su, How to design proper p -spacer order of the D- p -A dyes for DSSCs ? A density functional response, *Dye. Pigment.*, 2012, **95**, 313–321.

5 S. J. Sharma and N. Sekar, Charge Transfer as Bridging Correlator for DSSC Efficiency and NLO Property, *ChemistrySelect*, , DOI:10.1002/slct.202203262.

6 N. N. Ayare, S. Sharma, K. K. Sonigara, J. Prasad, S. S. Soni and N. Sekar, Synthesis and computational study of coumarin thiophene-based D- π -A azo bridge colorants for DSSC and NLOphoric application, *J. Photochem. Photobiol. A Chem.*, 2020, **394**, 112466.

7 J. Romiszewski, Z. Puterová-Tokarová, J. Mieczkowski and E. Gorecka, Optical properties of thiophene-containing liquid crystalline and hybrid liquid crystalline materials, *New J. Chem.*, 2014, **38**, 2927–2934.

8 S. L. Broman, S. L. Brand, C. R. Parker, M. Å. Petersen, C. G. Tortzen, A. Kadziola, K. Kilsa and M. B. Nielsen, Optimized synthesis and detailed NMR spectroscopic characterization of the 1,8a-dihydroazulene-1,1-dicarbonitrile photoswitch, *Arkivoc*, 2011, **2011**, 51–67.

9 W. W. Wardakhan, H. Z. Shams and H. E. Moustafa, Synthesis of polyfunctionally substituted thiophene, thieno[2,3-b]pyridine and thieno[2,3-d]pyrimidine derivatives, *Phosphorus, Sulfur Silicon Relat. Elem.*, 2005, **180**, 1815–1827.